XLIII CILAMCE
21–25, November, 2022
FOZ DO IGUAÇU – PR – BRAZIL

Representative computational mechanical simulation of a penstock reinforced transition block

Marco André Argenta[1]

[1]*Dept. of Civil Construction, Federal University of Paraná*
Av. Cel. Francisco H. dos Santos, 100, 81530-000, Paraná, Brasil
marco.argenta@ufpr.br

Abstract. This work describes the numerical-computational mechanical simulation of a hydroelectric plant water intake (penstock) transition block, in reinforced concrete, evaluated according to the premises of ABNT NBR 6118/2014 standard. The computational mechanical simulation performed, based on the finite element method (FEM), discretized the block in three-dimensional tetrahedral solid elements and the reinforcement in three-dimensional single-line elements. Author based the analysis on loads in service, i.e., safety coefficients have not been used to reduce the resistance of the material or to increase the self-weight and hydrostatic loads. Author have carried out a results analysis of the block concrete using the Willam-Warnke criterion of failure. In the reinforcement, author have used the safety factor as a function of the resistance of each bar. The results showed the block has enough structural integrity to not suffer structural failures in service.

Keywords: Penstock, Finite elements, Simulation, Dams, Reinforced concrete

1 Introduction

The numerical-computational mechanical model and simulation object described in this work is a hydroelectric plant penstock transition block, evaluated according to the premises of ABNT NBR 6118/2014 item 14.8.2 ([1]). It is located at the water intake, which is a part of the dam, one at each penstock. The penstock blocks consist of three units of 20.50 m each separated by contraction joints. Built in the year 2006 with reinforced concrete, these three transition blocks used f_{ck} of 18 MPa and CA-50 steel with different diameters.

2 Methodology

Author carried out the mechanical simulation with three loads acting on the block: the self-weight (PP), the hydrostatic weight (PH), considering the water level at the maximum reservoir level and equivalent overpressure load 1.2x (20% higher) the value of hydrostatic weight caused by quick closing of the machine (PH20).

Author considered two simple combinations (direct sum of effects): combination C1 with the self-weight (PP) acting together with the maximum hydrostatic weight of the reservoir (PH) and combination C2 with the self-weight (PP) with the overpressure by quick closing of the machine (PH20).

Author based the analysis on loads in service, i.e., safety coefficients are not used to reduce the resistance of the material involved or increase the self-weight or hydrostatic loads.

Based on the finite element method (FEM), the computational mechanical simulation performed discretized the block in three-dimensional tetrahedral solid elements and the reinforcement in three-dimensional single-line elements, considering the block joint regions with zero displacements.

Author used convergence controls and mesh connectivity to ensure good numerical results and the association of distinct elements.

All nodes on the inner faces of the block transition region received a nodal load relative to 1/6 hydrostatic pressure (PH) in the element, calculated relative to the water level at the maximum reservoir level, according to the equation $p_h = \rho \times g \times h$, where p_h is the hydrostatic pressure, ρ is the fluid density, g is the acceleration of gravity and h is the height of the pressure position p_h relative to the Y-axis.

Author calculated the height h as the distance in y, vertical, from the face geometric center of each transition region exposed element to the water level at the maximum reservoir level. Author consider the fluid density as

1000 kg/m3 and the gravity acceleration as 9.81 m/s2.

Author applied the resulting pressure from the element's face across its entire area in the normal direction to the face, directed away from the transition (into the block). Author did the discretization for the nodes by multiplying this value by the area of the element face exposed to the transition region A_{fe}, resulting in a face resultant load that is divided by the number of element respective face nodes to be applied to each node $F_h = 1/6 \times p_h \times A_{fe}$.

Author added together values of loadings on the nodes of contiguous elements with concurrent nodes on an edge.

With the model and concrete simulation being three-dimensional, with volumes discretized into tetrahedral elements, each Gauss point (finite element superconvergent stress points) have 6 stress components, 3 normal stress, and 3 shear stress. This makes it somewhat complex to assess how close each point is to the rupture. Therefore, for the analysis of the results in the block concrete part, the author used the Willam-Warnke failure criterion [2]. Author chose it because the criterion applies to concrete, considers different tensile and compressive strengths, and takes into account the three-dimensional effect and the confinement effect. This criterion uses the 6 stress components already calculated as input and returns the value of a safety factor. This safety factor indicates safe concrete between values of 0.0 and 1.0 and concrete with possible failures for values above 1.0.

In addition to the 6 stress components, the criterion also needs the values of the concrete compressive, tensile, and biaxial stress strengths. The relationship between the concrete axial compressive strength (σ_c) and its biaxial strength (σ_b) author took from the literature, being adopted as [3]:

$$\beta = \frac{\sigma_b}{\sigma_c} \approx 1.14 \tag{1}$$

According to ABNT NBR 6118/2018 [1] for class C18 concrete, with characteristic compressive strength $f_{ck} = 18\ MPa$, used in the project, the compressive strengths (σ_c) and the tensile mean (σ_t) are:

$$\sigma_c = 18\ MPa \tag{2}$$

$$\sigma_t = 0.3\sqrt[3]{{f_{ck}}^2} \approx 2.06\ MPa \tag{3}$$

Thus, using the equation 1, the biaxial strength of this concrete is:

$$\sigma_b = 20.52\ MPa \tag{4}$$

With these values, author applied the failure criterion to the block concrete with a load combination of self-weight with hydrostatic pressure (C1) and self-weight with overpressure by quick closing of the machine (C2), in a direct sum without any weighting or factoring coefficients.

The Willam-Warnke failure criterion is calculated with the equation:

$$S_c = \frac{1}{\sigma_c}\sqrt{\frac{2}{15}}\frac{1}{r(\theta)}\sqrt{3J_2} + b_W I_1 \tag{5}$$

being $r(\theta)$ the radius in polar coordinates that indicates the stress surface of the deviatoric plane, J_2 the second invariant of the deviatoric part of the stress tensor, I_1 the first invariant of the stress tensor, and b_W the weighting parameter of the first invariant, calculated as:

$$b_W = \frac{\sigma_b - \sigma_t}{3\sigma_b\sigma_t} \tag{6}$$

The criterion obtains the value of $r(\theta)$ by:

$$r(\theta) = \frac{u(\theta) + v(\theta)}{w(\theta)} \tag{7}$$

being:

$$u(\theta) = 2r_c(r_c^2 - r_t^2)cos\left(\theta + \frac{\pi}{6}\right) \tag{8}$$

$$v(\theta) = r_c(2r_t - r_c)\sqrt{4(r_c^2 - r_t^2)cos\left(\theta + \frac{\pi}{6}\right)^2 + 5r_t^2 - 4r_t r_c} \tag{9}$$

$$w(\theta) = 4(r_c^2 - r_t^2)cos\left(\theta + \frac{\pi}{6}\right)^2 + (r_c - 2r_t)^2 \tag{10}$$

Which are a function of the radius in compression (r_c) and in tension (r_t) of the failure surface deviatoric trace:

$$r_c = \sqrt{\frac{6}{5}} \frac{\sigma_b \sigma_t}{3\sigma_b \sigma_t + \sigma_c(\sigma_b - \sigma_t)} \tag{11}$$

$$r_t = \sqrt{\frac{6}{5}} \frac{\sigma_b \sigma_t}{\sigma_c(2\sigma_b + \sigma_t)} \tag{12}$$

These radius must satisfy the relationship $rt > rc/2$, otherwise, the criterion does not apply.

Author evaluated the reinforcements by the safety factor between the resulting axial force in each element relative to the strength of each steel bar. As they are CA-50 steel bars with a yield strength of 500 MPa and a simplified uniform diameter of 20 mm, author calculated the safety factor for these bars (S_b) by:

$$S_b = 4\frac{N_s}{\pi \times 0.02^2 \times 500 \times 10^6} = \frac{N_s}{628320} \tag{13}$$

being N_s the axial force required for combinations C1 or C2.

2.1 Simulation procedure

The characteristics and idealizations of computational mechanical simulation are: a mechanical model of static loading; Linear relationship of stress and deformation of materials within the elastic regime; first-order strain and displacement relation; material components of the geometry structures considered are simply homogeneous and isotropic; all geometries in a single model, discretized in finite elements with matching edges and contiguous faces; boundary conditions of prescribed displacements equal to zero; self-weight loads on all elements and hydrostatic loads in specific positions and considered applied in a single time, representative of the critical post-filling operational period (maximum reservoir level).

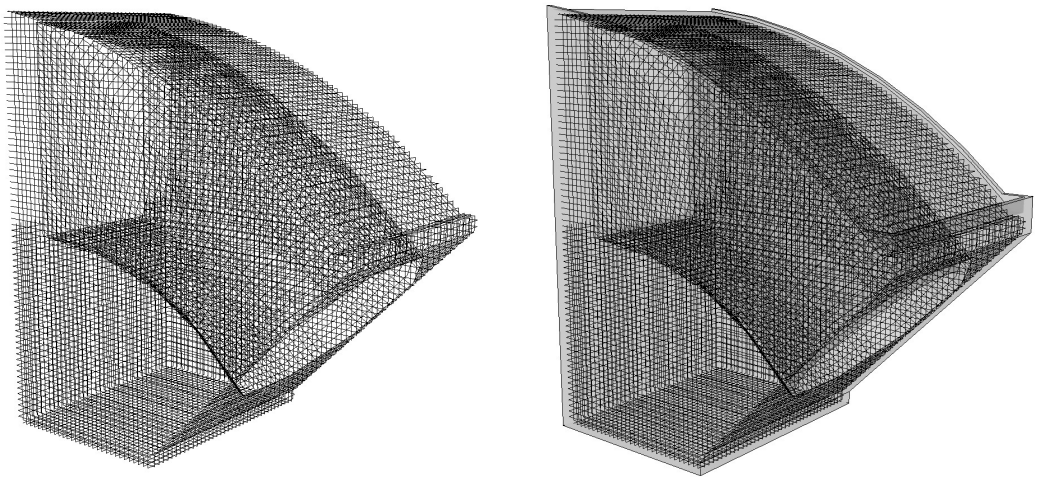

(a) (b)

Figure 1. (a) Complete reinforcements three-dimensional geometry, (b) Block with reinforcements.

The three-dimensional geometry of the model, the solid part of the block and the reinforcements, author have built with the help of the open-source software Salome version 9.6.0 [4], freely distributed with the general public license of the LGPL computational library (https: //opensource.org/licenses/LGPL-2.0) that provides a generic pre- and post-processing platform for numerical simulation, which, in this case, author used only the geometry generation part. The volume of the block has joined and embedded the block and transition reinforcements to start the process of geometries' discretization in solid and single-line finite elements.

Author obtained finite element meshes using the NETGEN mesh generator, part of the open-source NETGEN/NGsolve [5] package developed by the Vienna University of Technology, University of Göttingen, Germany,

Portland State University, RWTH Aachen University, and Johannes Kepler University, Linz, that is freely distributed. Process used the algorithm of free volumes, one-dimensional, two-dimensional to three-dimensional, with edges divided into segments and faces into triangles that run through the interior forming a 10-node isoparametric quadratic tetrahedron with three degrees of freedom of displacement per node. Numerical integration used the 5-point rule of integration of the Gaussian quadrature to allow more accurate stress results in their locations within the elements. Initially, elements hypothesis assumed 100 cm maximum size approximately, with 7 steps optimization on the volume mesh to avoid excessively distorted elements, mainly in the coupling regions with the reinforcement representative lines. This initial hypothesis generated a total of 612,423 nodes in 392,401 block elements. After the geometry adjustment, author refined and adapted the mesh to the places that needed coupling with the reinforcement lines. The final mesh, after the convergence process, resulted in 1,127,371 nodes from 849,625 elements in the block (Figure 2).

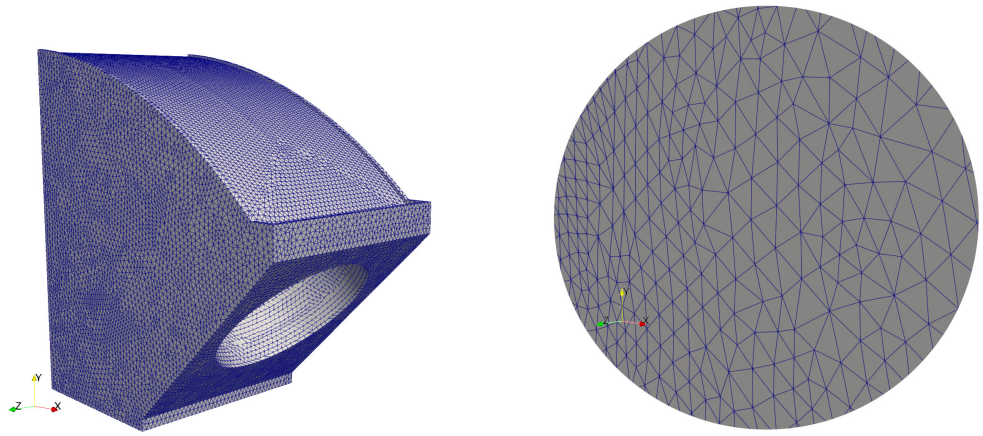

(a) (b)

Figure 2. (a) Block geometry discretization in finite elements, (b) Approximation on the discretized surface.

Author chose the three-dimensional truss element with 2 nodes with linear interpolation and 3 degrees of freedom of displacement per node for the discretization of the representative lines of the reinforcements. This choice took into account the possibility of coupling between its degrees of freedom and the degrees of freedom of the tetrahedral element used, in addition to its applicability to simulate the reinforcement in reinforced concrete. The discretization followed the result of the tetrahedral element convergence with the division of the representative lines of the reinforcements according to the block element edges in the regions with required compatibility. This procedure resulted in 90,568 nodes with 52,520 truss elements (Figure 3).

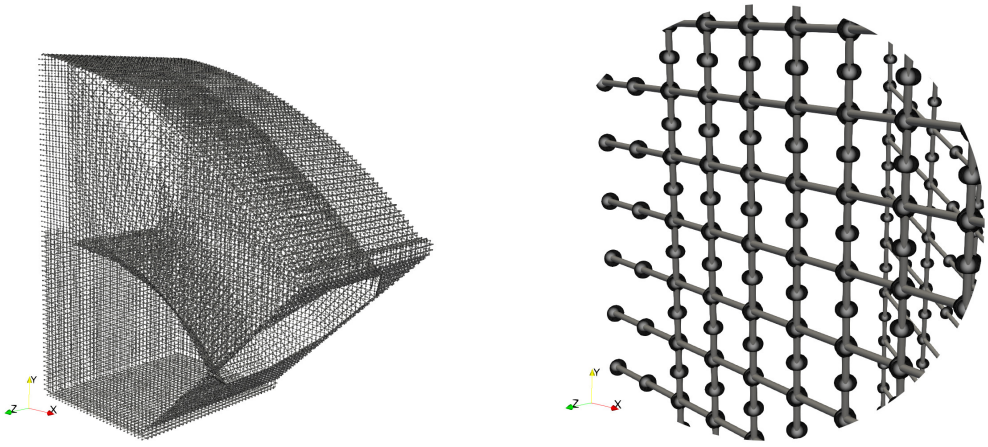

(a) (b)

Figure 3. (a) Reinforcement geometry discretization in finite elements, (b) Approximation on the discretized reinforcement.

Author had achieved mesh convergence through H-type refinement (decreased element size), also with the aid of NETGEN, with a sequential reduction of the edges of tetrahedral elements size and the finite element method

primary variables monitoring, i.e., the displacements. I have made the reduction until the result of previous pass displacements approached the current pass result, within the tolerance of 0.01 mm for all nodes in the model.

The mesh connectivity, responsible for coupling the effects of different elements, in the case of the tetrahedral elements with the truss elements, got done with a search and replacement of the tetrahedral elements' mesh nodes by the truss elements overlapping ones according to the identical coordinates. In the end, the number of nodes in the model resulted in 1,179,892.

All mesh nodes received a vertical load directed downwards with the value of 1/10 of the weight of their respective tetrahedral elements and 1/2 in each node in the truss elements, relative to their own weight (PP), calculated according to the densities of each material, according to the table 1. In concurrent nodes between neighboring elements, author have summed these loads. The acceleration due to gravity has been considered being 9.81 m/s2.

Table 1. Physical and mechanical properties of materials for simulation.

Material	**Density [kg/m3]**	**Elastic modulus [MPa]**	**Poisson's coefficient**
Concreto	2400	23759	0,20
Aço	7850	210000	0,30

The nodes of the elements' faces in the vertical block/dam support region and horizontal block/dam support region author defined with prescribed displacements of zero values in all their degrees of freedom, simulating a completely fixed support in these regions.

The equivalent overpressure loading by quick closing of the machine (PH20) author considered being 20% greater than the hydrostatic weight value and author determined by multiplying the calculated values of F_h for each model node in the inner part of the region of transition by 1.2.

The mechanical properties necessary for the simulation of the materials involved, CA-50 steel and concrete $f_{ck} = 18$ MPa, author defined according to ABNT NBR-6118/2014 [1] and their values are present in the table 1.

The concrete elastic modulus E_c author approximated by the expression $E_c = \alpha_e \times 5600\sqrt{f_{ck}}$ with $\alpha_e = 1.0$, idealizing the aggregates as originating from gneiss or granite and $f_{ck} = 18$ MPa.

The author of this work developed routines for computational mechanical simulations in finite elements in C++ and python, which are his intellectual property [6].

The results author wrote in VTK format [7] (Visualization Toolkit, free and open-source software for visualizing scientific data) and the images generated with the help of Paraview v5.9 [8] (code application free and open-source for data analysis and visualization), also freely distributed.

3 Results

Author present simulation results in this section for combinations C1 and C2. The values obtained for the Willam-Warnke failure criterion for the concrete of the block are show in the figure 4 for the combination C2, which turned out to be the critical combination.

From this figure, from the C2 combination, with the overpressure load combined with the own weight, one can observe high factors in general, but with a good part of the block still well in favor of safety, with factors below 0.5. Author draw attention to the outer lateral regions of the block with factors between 0.5 and 0.9 and the lower inner sides of the transition region and the center superior to the end of the block, with factors between 0.5 and 0.8. There is a clear concentration of stress on the sides of the block in the rectangular region of the transition coupled to the dam body, with factors between 0.7 and 1.2 in a small range.

The high factors of the small band in the rectangular region of the transition that is coupled to the body of the dam and that author considered its face in the model as embedded should not be of concern (Figures 4b. The values of the numerical model are approximate and everybody knows from the classical literature that the finite element method does not represent well regions of stress concentration, tending to have values much higher than those that occur. In these regions, this is the case, and author estimated using his experience that the real factor is between 0.7 and 0.8 on these edges.

Author concluded the same cannot be from the lateral external faces of the blocks, where a band of high factors runs along the wall in line with the curvature of the transition worsening in the region close to the end of the block connected with the conduit. This region is resulting in high factors due to the small thickness of the block between the transition and its external face, resulting in a region of little stiffness. One can observe the same in the reinforcement of this region, which contributes considerably to reducing displacement and stresses in the

concrete in this small thickness, but not enough to keep the factors low. The axial forces in the reinforcement author illustrated in figures 5a and 5a for combinations C1 and C2, respectively.

With the equation 13, using the absolute maximum critical values of the figure 5 for the combinations C1 (2778.7 N) and C2 (3663.0 N), author arrive at a safety factor for reinforcement in combination C1, S_{C1} and combination C2, S_{C2} of:

$$S_{C1} = 0,0044 \tag{14}$$

$$S_{C2} = 0,0058 \tag{15}$$

These results make it very clear that the reinforcements are little requested, because, even with the simplifications adopted in the model, the values of their maximum safety factors are low.

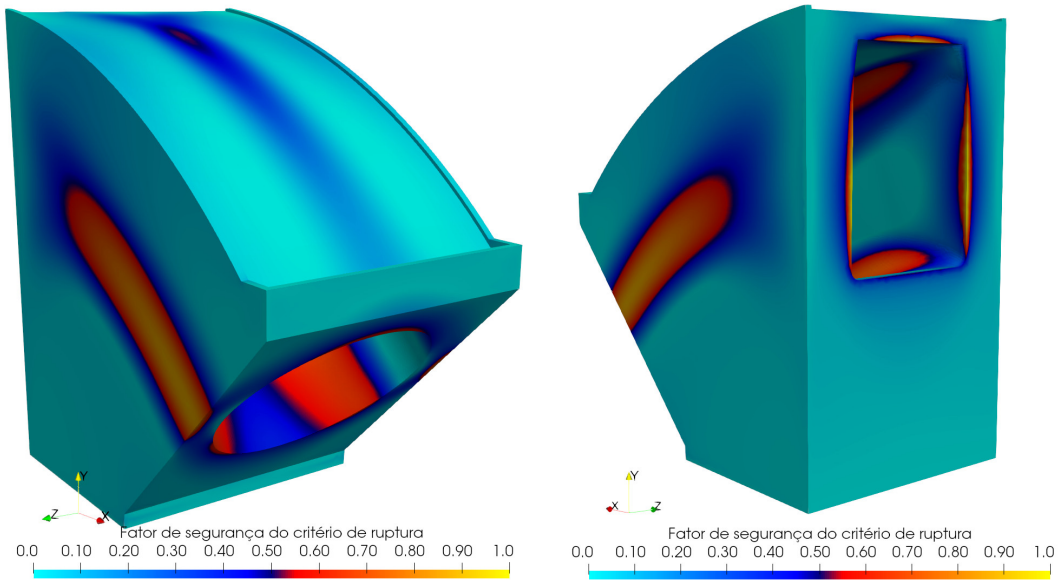

(a) (b)

Figure 4. Failure criterion safety factor values (a) isometric anterior view, (b) isometric posterior view, for the C2 combination of PP with PH20.

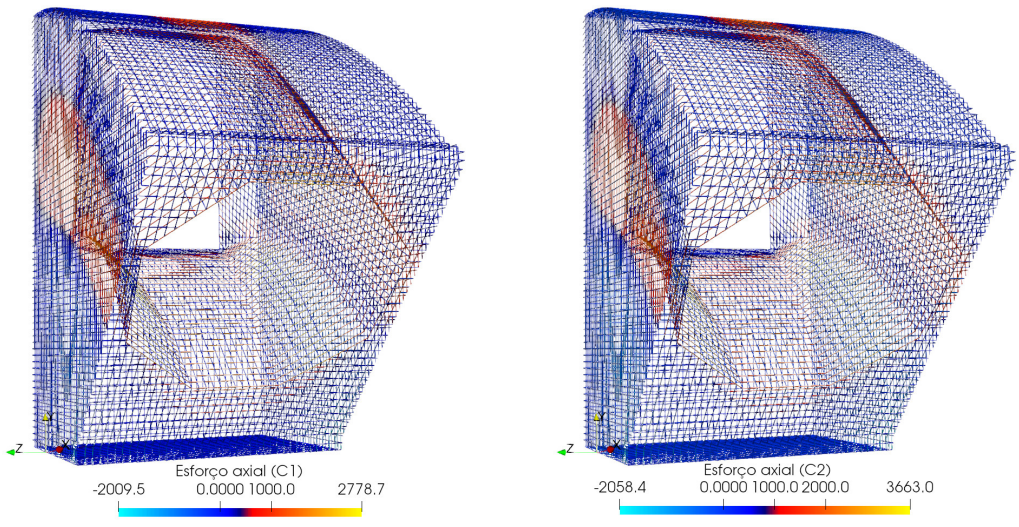

(a) (b)

Figure 5. Axial forces in reinforcements [N] (a) isometric anterior view for combination C1, (b) anterior isometric view for combination C2.

4 Conclusions

According to the results and analysis of the computational simulation, author drawn some conclusions regarding the mechanical behavior of the transition block of the model: author considered the numerical results obtained satisfactory for the conditions imposed in the mechanical simulation; the reinforcement simplifications in no way influenced the critical region on the outer sides of the block, as the reinforcement is practically identical to the design region; Author suggest attention to the external lateral regions of the block with high safety factors (Figure 4) because, due to the lack of transverse rigidity of the concrete, they may, over time, present excessive external cracking and/or leaks; the reinforcement has very low tension, far from the yielding of the steel in the most stressed bars, and, according to ABNT NBR 6118/2018, the safety of a reinforced concrete piece must consider the ductile rupture due to the elongation of the reinforcement, or that is, the most requested reinforcements must reach the yield level before the concrete reaches its rupture, which is not the case in the critical region of small thickness of the block; In general, the results indicate that the block has enough structural integrity to not suffer structural failures in service.

Acknowledgements. The author would like to acknowledge his family's patience while he programmed this simulation.

Authorship statement. The authors hereby confirm that they are the solely liable persons responsible for the authorship of this work and that all material that has been herein included as part of the present paper is either the property (and authorship) of the authors or has the permission of the owners to be included here.

References

[1] ABNT. Nbr 6118: Projeto de estruturas de concreto - procedimento, 2014.
[2] K. J. William and E. Warnke. Constitutive model for the triaxial behavior of concrete, 1975.
[3] E. Chen and C. K. Y. Leung. Effect of uniaxial strength and fracture parameters of concrete on its biaxial compressive strength. *Journal of Materials in Civil Engineering*, vol. 26, n. 6, pp. 06014001, 2014.
[4] OPENCASCADE, CEA/DEN, and R&D. Open-source software that provides a generic pre and post-processing platform for numerical simulation, 2020.
[5] J. Schöberl. Netgen an advancing front 2d/3d-mesh generator based on abstract rules. *Computing and Visualization in Science*, vol. 1, n. 1, pp. 41–52, 1997.
[6] M. A. Argenta. Método dos elementos finitos aplicado à engenharia de estruturas, 2011.
[7] W. Schroeder, K. Martin, B. Lorensen, and I. Kitware. *The Visualization Toolkit: An Object-oriented Approach to 3D Graphics*. Kitware, 2006.
[8] Sandia National Labs, Kitware Inc, and Los Alamos National Labs. Paraview: Parallel visualization application, 2020.